

Binary Lenses in OGLE-III EWS Database. Seasons 2002–2003

M. Jaroszyński¹, A. Udalski¹, M. Kubiak¹, M. Szymański¹,
G. Pietrzyński^{1,2}, I. Soszyński¹, K. Żebruń¹,
O. Szewczyk¹ and Ł. Wyrzykowski¹

¹Warsaw University Observatory, Al. Ujazdowskie 4, 00-478 Warszawa, Poland
e-mail:(mj,udalski,mk,msz,pietrzyn)@astrouw.edu.pl
(soszynsk,zebrun,szewczyk,wyrzykow)@astrouw.edu.pl

² Universidad de Concepción, Departamento de Física, Casilla 160-C,
Concepción, Chile
e-mail: pietrzyn@hubble.cfm.udec.cl

ABSTRACT

We present 15 binary lens candidates from OGLE-III Early Warning System database for seasons 2002–2003. We also found 15 events interpreted as single mass lensing of double sources. The candidates were selected by visual light curves inspection. Examining the models of binary lenses of this and our previous study (10 caustic crossing events of OGLE-II seasons 1997–1999) we find one case of extreme mass ratio binary ($q \approx 0.005$) and the rest in the range $0.1 < q < 1.0$, which may indicate the division between planetary systems and binary stars. There is no strong discrepancy between the expected and the observed distributions of mass ratios and separations for binary stars.

Gravitational lensing – Galaxy: center – binaries: general

1 Introduction

In this article we present the results of the search for binary lens events among microlensing phenomena discovered by the Early Warning System (EWS – Udalski *et al.* 1994b, Udalski 2003) of the third phase of the Optical Gravitational Lens Experiment (OGLE-III) in seasons 2002–2003. This is the continuation of the study of seasons 1997–1999 presented by Jaroszyński (2002, hereafter Paper I).

As estimated by Mao and Paczyński (1991) several percent of all microlensing events in our Galaxy should be caused by binary systems of stars acting as lenses. In the same paper the analysis of microlensing events caused by planetary systems is proposed as a way of discovering extra-solar planets. The sufficiently large database of binary and/or planetary microlensing events may serve as an independent tool of studying such systems. Some basic ideas for binary lens analysis can be found in the review article by Paczyński (1996).

Lensing by two point masses has been studied by Schneider and Weiss (1986). Various aspects of binary lens modeling have been described (among others) by Gould and Loeb (1992), Bennett and Rhie (1996), Gaudi and Gould (1997), Dominik (1999), Albrow *et al.* (1999c), and Graff and Gould (2002).

The first microlensing phenomenon interpreted as being due to the binary system was the event OGLE-7 (Udalski *et al.* 1994a). Several binary lens events with good light curve coverage were used to study the atmospheres of the source stars (*e.g.*, Albrow *et al.* 1999b) or to constrain the lensing system parameters (*e.g.*, Albrow *et al.* 1999a). The first lens mass measurement was obtained by An *et al.* (2002) based on a binary lens event with combined effects of parallax motion and caustic crossing. The systematic study of 21 binary lens events found in MACHO data was presented by Alcock *et al.* (2000).

Paper I presents the analysis of 18 binary lens events found in OGLE-II data reduced with difference photometry, DIA, (Alard and Lupton 1998) by Woźniak (2000) and Woźniak *et al.* (2001). The aim of the present study is similar. The combined sample of events showing caustic crossings (10+15 events in OGLE-II and OGLE-III to date) is large enough for a crude statistical analysis of the binary lens population.

In the next Section we describe the selection of binary lens candidates. In Section 3 we describe the procedure of fitting models to the data. The results are described in Section 4, and the discussion follows in Section 5. The extensive graphical material is shown in Appendices.

2 Choice of Candidates

The OGLE-III data are routinely reduced with difference photometry (DIA) which gives high quality light curves of variable objects. The EWS system of OGLE-III (Udalski 2003) automatically picks up candidate objects with microlensing-like variability.

There are 389/462 microlensing events candidates selected by EWS in 2002/2003 seasons. We visually inspected all candidate light curves looking for features characteristic of binary lenses (multiple peaks, U-shapes, asymmetry). We avoided light curves showing excessive noise. We selected 8/16 candidate events in 2002/2003 data for further study.

This work is a continuation of Paper I, where we have introduced some criteria to obtain a sample of high S/N ratio microlensing light curves among transient events. Following this approach we find the average base flux of each light curve and its standard deviation δ . It may include also a small amplitude intrinsic source variability and is usually higher than the averaged observational error obtained during photometric data reduction. We rescaled all observational errors by the factor $s \equiv \delta / \langle \sigma_i \rangle_{\text{base}}$ calculated for the unlensed part of the light curve. In Paper I we considered only light curves with at least 7 high flux (*i.e.*, $\geq 5\delta$ above the base) measurements. We relax this requirement here, when constructing a single mass lens sample, which includes events with at least 5 points 5δ above the base flux. For the single lens sample we also require a reasonably good fit, postulating $\chi^2/\text{DOF} \leq 2$. There are 268 single lens events in 2002/2003 data passing these criteria. Three of the binary lens candidates do not have the required number of high flux measurements.

3 Fitting Binary Lens Models

The models of the two point mass lens were investigated by many authors (Schneider and Weiss 1986, Mao and DiStefano 1995, DiStefano and Mao 1996, Dominik 1998, to mention only a few). The effective methods applicable for extended sources have recently been described by Mao and Loeb (2001). While we use mostly the point source approximation, we extensively employ their efficient numerical schemes for calculating the binary lens caustic structure and source magnification.

We fit binary lens models using the χ^2 minimization method for the light curves. It is convenient to model the flux at the time t_i as:

$$F_i = F(t_i) = A(t_i) \times F_s + F_b \quad (1)$$

where F_s is the flux of the source being lensed, F_b is the blended flux (from the source close neighbors and possibly the lens), and the combination $F_b + F_s = F_0$ is the total flux, measured long before or long after the event. The lens magnification (amplification) of the source $A(t_i) = A(t_i; p_j)$ depends on the set of model parameters p_j . Using this notation one has for χ^2 :

$$\chi^2 = \sum_{i=1}^N \frac{(A_i F_s + F_b - F_i)^2}{\sigma_i^2} \quad (2)$$

where σ_i are the rescaled errors of the flux measurement taken from the DIA photometry. The dependence of χ^2 on the binary lens parameters p_j is complicated, while the dependence on the source/blend fluxes is quadratic. The subset of equations $\partial\chi^2/\partial F_s = 0$; $\partial\chi^2/\partial F_b = 0$ can be solved algebraically, giving $F_s = F_s(p_j; \{F_i\})$ and $F_b = F_b(p_j; \{F_i\})$ thus effectively reducing the dimension of the parameter space. In some cases this approach may give unphysical solutions with negative blended flux ($F_b < 0$). Using the fluxes (F_s, F_b) as independent parameters may help avoiding such problems, and we do it in a part of calculations. In particular we always use this method when modeling single lens events needed for comparison.

Binary lens models are possibly and typically non unique (Dominik 1999). The presence of caustics and cusps in the lens theory (Schneider, Ehlers and Falco 1992, Blandford and Narayan 1992) makes the χ^2 dependence on the model parameters complicated and discontinuous for point sources. For extended sources the discontinuities in strict mathematical sense are not present, but the χ^2 surface remains complex, possessing large number of local minima and deep narrow valleys, which makes the search for minima complicated. For this reason we combine the scan of the parameter space and the random choice of initial parameters with the standard minimization techniques in our search.

For most of the light curves we investigate, the caustic crossings are not well sampled, and we are forced to use a point source approximation in the majority of our models. In two cases (events OGLE 2003-BLG-170 and OGLE 2003-BLG-267) the caustic crossings are resolved, so the extended source models can be fitted. In these cases the strategy resembling Albrow *et al.* (1999c) for finding binary lens models can be used. It is based on the fact that some of the parameters (source angular size, strength of the caustic) can be fitted independently, so for an initial fit one can split the parameter space into two lower dimensionality sub-manifolds.

A binary system consists of two masses m_1 and m_2 , where by convention $m_1 \leq m_2$. The Einstein radius of the binary lens is defined as:

$$r_E = \sqrt{\frac{4G(m_1 + m_2)}{c^2} \frac{d_{OL}d_{LS}}{d_{OS}}} \quad (3)$$

where G is the constant of gravity, c is the speed of light, d_{OL} is the observer–lens distance, d_{LS} is the lens–source distance, and $d_{OS} \equiv d_{OL} + d_{LS}$ is the distance between the observer and the source. The Einstein radius serves as a length unit and the Einstein time: $t_E = r_E/v_\perp$, where v_\perp is the lens velocity relative to the line joining the observer with the source, serves as a time unit. The passage of the source in the lens background is defined by seven parameters: $q \equiv m_1/m_2$ ($0 < q \leq 1$) – binary mass ratio, d – binary separation expressed in r_E units, β – angle between the source trajectory as projected onto the sky and the projection of the binary axis, b – impact parameter, t_0 – time of closest approach of the

source to the binary center of mass, t_E – Einstein time, and r_s – source radius. Thus we are left with the seven or six dimensional parameter space, depending on the presence/absence of observations covering the caustic crossings.

We begin with a scan of the parameter space using a logarithmic grid of points in (q, d) plane ($10^{-3} \leq q \leq 1$, $0.1 \leq d \leq 10$) and allowing for continuous variation of the other parameters. The choice of starting points combines systematic and Monte Carlo searching of regions in parameter space allowing for caustic crossing or cusp approaching events. The χ^2 minimization is based on downhill method and uses standard numerical algorithms. When a local minimum is found we make a small Monte Carlo jump in the parameter space and repeat the downhill search. In some cases it allows to find a different local minimum. If it does not work several times, we stop and try next starting point.

Minimizations with fixed physical binary parameters serve mostly to obtain $\chi^2(q, d)$ maps showing the preferred binary models. We perform also minimizations in higher dimensions, including mass ratio, binary separation, source flux and blended flux as independent parameters. This improves the models, since now no variables are limited to grid values only. Even more important is the fact that in a higher dimension space there may exist a downhill path joining two points impossible in a lower dimension subspace. The $\chi^2(q, d)$ maps are improved during high dimension minimization: whenever the running value of χ^2 is lower than the value assigned to the closest grid point, we exchange them. The maps shown in Appendix 1 are obtained as a result of such a procedure.

Only the events with characteristics of caustic crossing (apparent discontinuities in observed light curves, U-shapes) can be treated as safe binary lens cases. The double peak events may result from cusps approaches, but may also be produced by double sources (*e.g.*, Gaudi and Han 2004). In such cases we also check the double source fit of the event postulating:

$$F(t) = A(u_1(t)) \times F_{s1} + A(u_2(t)) \times F_{s2} + F_b \quad (4)$$

where F_{s1} , F_{s2} are the fluxes of the source components, F_b is the blended flux, and $A(u)$ is the single lens amplification (Paczynski 1986). The dimensionless source – lens separations are given as:

$$u_1(t) = \sqrt{b_1^2 + \frac{(t-t_{01})^2}{t_E^2}} \quad u_2(t) = \sqrt{b_2^2 + \frac{(t-t_{02})^2}{t_E^2}} \quad (5)$$

where t_{01} , t_{02} are the closest approach times of the source components, b_1 , b_2 are the respective impact parameters, and t_E is the (common) Einstein time.

4 Results

In Table 1 we show the results of binary lens fitting for a long list of events. Some of them are "strong cases", which we denote by "b" (for binary) in the third column. Other may be better interpreted as single mass lensing of double sources, which we denote by "d". If binary lens and double source models have similar formal quality, but the binary light curve has caustic crossings and/or cusp approaches in places not covered by observations, we choose the double source model.

Columns 1–2 give the event identification (year and EWS number), the fourth column gives χ^2 and DOF (degrees of freedom) number, and the other columns give the parameters for the best models of each of the events. In some

cases we include also another solution if it belongs to a distinct χ^2 minimum and lies inside the confidence region. Our best fits are also shown on the plots in Appendix 1. For each binary there are three separate plots. The first shows the source trajectory as projected onto the lens plane with caustic structure and binary components included. The model light curves and observed magnitudes are shown in the second plot. Third diagram shows χ^2 confidence regions in the $\lg q$ - $\lg d$ plane.

Table 1
Parameters of binary lens modeling

Year	Event		χ^2/DOF	s	q	d	β	b	t_0	t_E	f	r_s
2002	051	b	110.0/ 58	1.45	0.943	1.390	96.71	-0.48	2391.4	88.1	0.87	
2002	069	b	1014./ 95	1.18	0.721	0.497	110.41	-0.02	2456.4	99.7	1.00	
2002	099	d	134.4/151	1.63	0.248	1.963	16.39	0.09	2413.0	34.4	0.37	
2002	114	b	77.5/ 80	1.80	0.745	0.623	83.13	-0.04	2412.5	75.8	0.12	
2002	135	d	170.3/159	1.34	0.144	0.398	42.28	0.06	2441.5	148.2	0.06	
		d	171.8/159	1.34	0.128	1.089	297.78	-0.44	2440.9	32.2	0.76	
		d	172.0/159	1.34	0.678	0.734	34.65	-0.33	2441.0	39.3	0.51	
2002	158	d	115.7/103	1.08	0.051	0.872	45.80	0.18	2467.9	56.5	0.69	
2002	256	d	171.3/110	1.22	0.081	1.066	315.79	0.15	2485.9	40.1	0.25	
2002	321	d	94.1/ 97	1.16	0.251	0.708	30.72	0.08	2523.9	50.9	0.96	
2003	021	b	131.2/121	1.42	0.799	0.941	57.91	-0.09	2776.8	54.9	0.96	
2003	056	b	147.5/120	1.78	0.743	1.497	318.72	-0.02	2764.8	40.3	0.79	
2003	084	d	110.1/103	1.65	0.794	0.794	85.34	-0.01	2697.3	124.8	0.51	
2003	124	b	128.0/122	1.25	0.666	0.959	72.57	-0.11	2768.7	73.0	0.27	
2003	135	b	59.5/110	3.55	0.129	0.847	123.00	-0.20	2724.3	339.9	0.06	
2003	170	b	161.1/149	1.46	0.789	1.213	133.66	-0.35	2794.1	15.6	0.75	0.0027
2003	194	d	117.2/112	1.24	0.692	3.357	157.24	0.77	2749.4	32.4	0.87	
		d	118.3/112	1.24	0.702	0.562	134.46	0.09	2804.4	21.8	0.91	
2003	200	b	90.8/105	1.51	0.209	1.495	122.70	-0.06	2836.4	46.0	0.54	
2003	235	b	151.1/175	1.19	0.005	1.128	318.91	-0.10	2848.2	75.0	0.58	
2003	236	b	125.4/122	1.32	0.175	0.838	196.36	-0.13	2801.5	73.8	0.12	
2003	260	b	127.2/120	1.38	0.112	2.269	288.48	-1.52	2968.7	272.3	0.10	
		b	129.6/120	1.38	0.488	1.845	106.77	-0.42	2840.7	139.4	0.05	
		b	129.8/120	1.38	0.450	0.624	256.90	-0.01	2827.8	106.7	0.04	
2003	266	d	88.6/ 98	1.38	0.448	1.071	246.51	0.02	2822.9	25.0	0.05	
2003	267	b	1042./250	1.23	0.628	0.352	87.88	-0.01	2845.3	88.8	0.37	0.0008
2003	291	b	325.3/159	1.45	0.837	3.457	198.53	0.48	2956.6	39.8	0.49	
2003	340	d	179.4/148	1.54	0.001	1.105	265.20	0.03	2900.9	208.4	0.15	
		d	179.9/148	1.54	0.049	1.447	153.99	-0.08	2904.0	106.6	0.42	
2003	380	b	85.3/118	1.29	0.615	0.784	169.05	0.14	2876.5	78.9	0.21	

Note: The table contains the year and the EWS event number, the event classification according to this study ("b" - for binary lens, "d" - for double source), the rescaled χ^2 value and the DOF number, the error scaling factor s ($\chi^2 = \chi_{\text{raw}}^2/s^2$), mass ratio q , binary separation d , source trajectory direction β , impact parameter b , time of passing by the center of mass t_0 , Einstein time t_E , and blending parameter $f = F_s/F_0$. The source radius r_s (in Einstein units), is given only in cases of events with well resolved caustic crossings.

In Table 2 we show the results of double source modeling. We include the ambiguous cases of binary lens / double source models as well as some events showing well separated, smooth maxima in their light curves, which may be safely treated as single mass lensing of double sources. The comparison of two kinds of fits is given in Appendix 2, and the well separated double source events are shown in Appendix 3.

T a b l e 2
Parameters of double source modeling

Year	Event	χ^2/DOF	s	b_1	b_2	t_{01}	t_{02}	t_E	f_1	f_2
2002	018	92.1/107	1.20	0.4495	0.4356	2351.09	2573.47	31.6	0.203	0.797
2002	099	134.2/151	1.63	0.0821	0.0294	2402.93	2425.23	47.1	0.147	0.051
2002	135	181.7/159	1.34	0.0394	0.0951	2432.39	2449.89	81.2	0.033	0.070
2002	158	120.8/103	1.08	0.0690	0.1934	2456.42	2472.80	60.2	0.065	0.543
2002	256	182.2/110	1.22	0.0025	0.0220	2471.92	2488.38	199.9	0.002	0.023
2002	321	90.6/ 97	1.16	0.0099	0.0261	2517.96	2524.34	61.9	0.071	0.553
2003	063	118.2/113	1.64	0.5878	1.6755	2748.84	2891.20	29.1	0.352	0.648
2003	067	113.4/114	1.48	0.5433	0.5792	2772.01	3077.06	66.8	0.386	0.470
2003	084	145.1/103	1.65	0.0894	0.0667	2717.20	2759.63	108.1	0.279	0.721
2003	095	112.7/108	2.39	0.2313	0.3403	2775.44	2881.33	44.4	0.273	0.327
2003	124	210.5/122	1.25	0.1068	0.0001	2751.10	2768.21	125.1	0.124	0.014
2003	126	137.1/108	1.97	0.1480	1.0042	2774.57	2830.57	14.9	0.820	0.180
2003	194	127.0/112	1.25	0.0000	0.2027	2802.66	2804.57	19.8	0.069	0.918
2003	266	119.1/ 98	1.39	0.2285	1.1596	2810.27	2825.33	10.4	0.223	0.777
2003	340	191.2/148	1.55	0.0649	0.0114	2900.11	2902.33	134.2	0.228	0.040

Note: The table contains the year and event number according to EWS, the rescaled χ^2 value and the DOF number, the error scaling factor s , the impact parameters b_1 and b_2 for the two source components, times of the closest approaches t_{01} and t_{02} , Einstein time t_E , and blending parameters $f_1 = F_{s1}/(F_{s1} + F_{s2} + F_b)$ and $f_2 = F_{s2}/(F_{s1} + F_{s2} + F_b)$.

For the further study of binary mass lensing we choose only the "safe" cases (denoted "b" in Table 1). We also use the binary lenses of Paper I, but we limit ourselves only to caustic crossing events. The cusp approach events of Paper I are typically not well constrained. Some of them would probably be better interpreted as double source events.

4.1 Distribution of Mass Ratios and Separations

For statistical study of binary lens properties we use 10 caustic crossing events of seasons 1997–1999 (Paper I) and 15 "safe" events of the present study. Three of the events considered have more than one model with similar quality of fits belonging to two or three different classes of binary lenses (close/intermediate/wide). In such cases we assign statistical weights w_{1st} , w_{2nd} , etc. to the models, assuming the relation:

$$\frac{w_{2nd}}{w_{1st}} = \exp\left(-\frac{\chi_{2nd}^2 - \chi_{1st}^2}{2}\right) \quad (6)$$

and similarly for the 3rd model of the same event if applicable. The histograms for the distributions of mass ratio q and binary separation d are shown in Fig. 1.

As can be seen in the left panel the majority of binary lenses has mass ratio in the range $0.1 < q < 1.0$, typical for binary stars. There is one strong case of extreme mass ratio binary, which may be considered a "planetary system", the event OGLE 2003-BLG-235/MOA 2003-BLG-53 described in detail by Bond *et al.* (2004). In Paper I we have reported 2 cases of extreme mass ratio binaries, but both belong to cusp approach cases, not considered here. One of the models of OGLE 2003-BLG-340 has an extreme mass ratio $q = 0.0014$, but the alternative model has $q = 0.049$, and the double source model is not excluded.

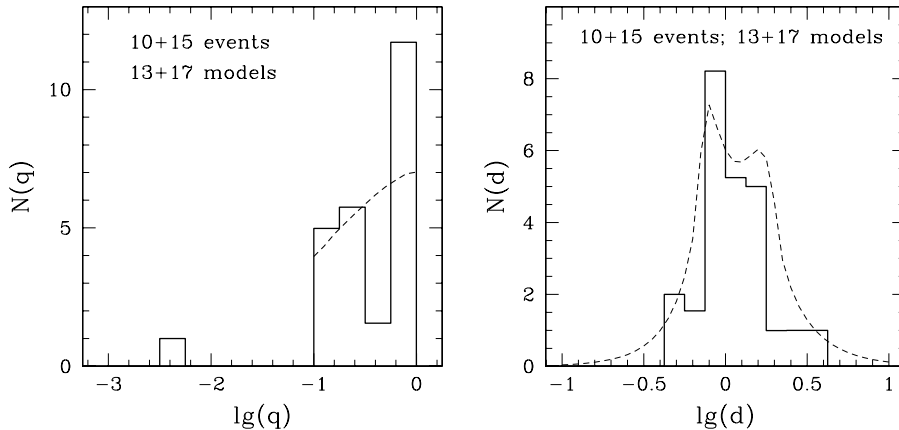


Fig. 1. Histograms showing the distribution of the mass ratio q (left) and the binary separation d (right) for the gravitational lens models (solid). Crude theoretical predictions of the distributions are plotted with dashed lines (see text for details). All binary lenses (seasons 1997–1999 and 2002–2003) are included.

We also show the predicted distributions of mass ratios and separations for the binary stars based on simplified assumptions. Following the approach of Mao and Paczyński (1991), based on Abt (1983) and Trimble (1990) (compare Paper I), we assume, that for the range $0.1 \leq q \leq 1$ the logarithms of the mass ratios of the binary stars and the logarithms of their semi-major axes are distributed uniformly:

$$P_{\text{bin}}(\lg q, \lg d) \sim \text{const.} \quad (7)$$

The observed distributions are influenced by the probability of given system to cause an observable binary lensing event. For a binary of known parameters and a source moving in a given direction the chance of crossing the caustic is proportional to its width perpendicular to the source trajectory. The size of caustic along the source trajectory is proportional to the time elapsing between caustic crossings, which also influences the probability of classifying the event as binary, but we neglect this effect as too difficult to model. Assuming that the observability of binary lens event is proportional to the chance of caustic crossing one has:

$$P_{\text{obs}}(\lg q, \lg d) \sim P_{\text{bin}}(\lg q, \lg d) \times w(\lg q, \lg d) \sim w(\lg q, \lg d) \quad (8)$$

where $w(\lg q, \lg d)$ is the caustic width averaged over all possible source path directions. Averaging over one of the parameters we obtain the one dimensional probabilities for finding a binary lens with a given mass ratio or separation, shown in Fig. 1 with dashed lines. No prediction is given for the planetary systems since there is no sufficient observational evidence to model the mass ratio distribution as in the case of binary stars.

The binary separation distribution has a strong peak around $d \approx 1$. Theoretically we predict two peaks at $d \approx 0.9$ and $d \approx 1.7$.

We apply the Kolmogorov – Smirnov test to the cumulative 1D distributions of binary mass ratios and separations. The postulated distribution of these parameters (Eqs. 7, 8) cannot be rejected.

4.2 Distribution of Events Duration

The Einstein time (t_E) can be found both for single and binary lenses. For comparison we also fit single events from OGLE-II and III databases. Not all fits are satisfactory. First we reject fits which have too high χ^2/DOF . Because of the parameter degeneracy in single lens fitting (Woźniak and Paczyński 1997) there remains a risk of including unphysical fits with formally good quality. Fits with very small impact parameters (large amplification) small source flux (small parameter f) and very long time scale belong to this category. To reject them we ignore all models with $f < 0.01$. We show histograms for single and binary events durations in Fig. 2.

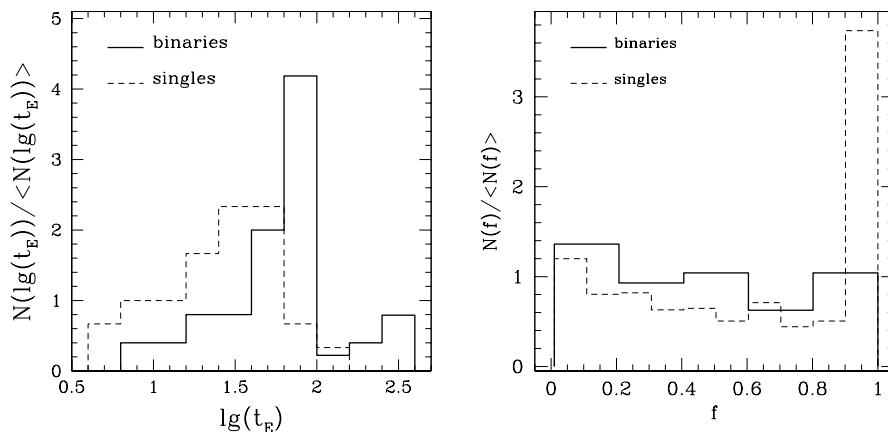


Fig. 2. Histograms showing the distributions of the Einstein time (left) and the blending parameter (right). Binary events (solid lines) and single events (dashed) are shown.

The durations of binary events are systematically longer as compared to single lens events. The binaries should be (on average) twice as massive as single lenses, so the binary events should be $\sqrt{2}$ times longer. The averaged logarithms of Einstein times for single/binary lens events in our sample correspond to event durations of $32^{\text{d}}/63^{\text{d}}$, in disagreement with the above estimate. The longer events have better chance of being classified as binary, but it is hard to estimate to what extent such selection effect explains the difference.

4.3 The Blending Parameter f

We show the distributions of blending parameter values for single and binary events. Again we neglect single lens models with $f < 0.01$, which removes most of the artifacts related to parameter degeneracy. Another problem – crowding of single mass fits with $f \approx 1$ and the unphysical models with $f > 1$ (compare Paper I) – is circumvented by inclusion of fluxes F_s and F_b as independent parameters of the fits. We put the histograms showing the distribution of blending parameter f in Fig. 2 for both single and binary lens models.

We also show the positions of binary and single lens models on a $\lg(t_E)$ – f diagram in Fig. 3. There is no apparent correlation between the parameters in the diagram, which means that the majority of parameter degeneracy artifacts have been removed. The crowding of points near upper boundary ($f = 1$) represents the bright sources which are not affected by blending.

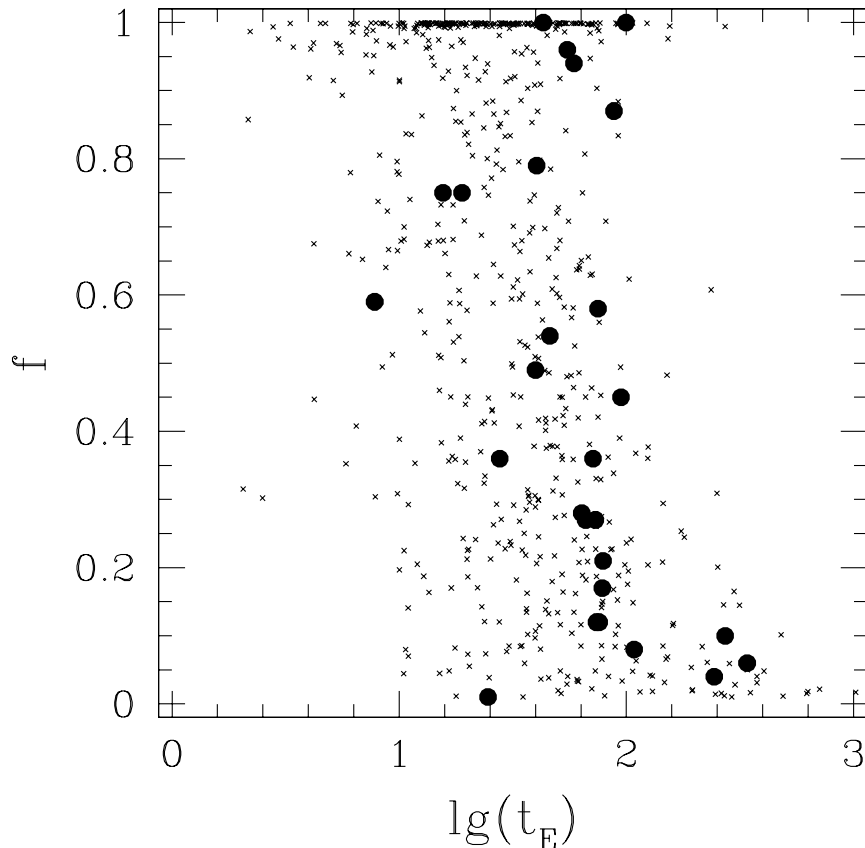


Fig. 3. The location of single lens (crosses) and binary lens models (large dots) on $\lg(t_E)$ - f plane. Events from seasons 1997–1999 and 2002–2003 are included.

5 Discussion

In this study (as in Paper I) we use rescaled errors when estimating the quality of fits *via* χ^2 test. The rescaling allows more adequate definition of confidence regions in parameter space and gives more reliable comparison between different fits. The linear scaling of all errors may be not adequate, since the relative accuracy of flux measurements is by far better for bright sources, and estimates based on the epochs when the source is faint may be not sufficient. Examining our models we also see that fits for the brightest sources are formally the worst.

For long lasting events the effects of binary and Earth orbital motions may be important, but we neglect both of them in this study. In general fits with more parameters require more observations during the event. In the case of caustic crossing events it is rather time between the crossings, not the Einstein time, which should be compared with the orbital period of binary/Earth to check whether their motion can influence the quality of our models. Finally, for strongly blended events ($f \ll 1$) the Einstein time is not a good measure of their duration, since the measurable changes in observed energy flux can be seen only when the amplification is really high. For single lens events the rough estimate of relevant time scale is given by ft_E . For binary events the intra-caustic time plays the role. All our models with extremely long duration ($t_E > 100^d$) are also strongly blended, and the introduction of extra parameters

in these cases is not promising. The event which certainly deserves improved modeling including parallax effect and/or binary rotation is OGLE 2003-BLG-267 ($t_E = 89^d$, $f = 0.37$), a case with well sampled caustic crossings and showing some systematic differences between observations and model (see Appendix 1). Similarly it is impossible to obtain a satisfactory model for OGLE 2003-BLG-291 without including some extra parameters. We are going to describe this event with more details elsewhere.

The main purpose of this study is the statistical characteristic of the population of binary lenses. The total number of “strong” binary lens cases (including those of Paper I) is still low (25). The distribution of our models in $(\lg q, \lg d)$ plane is in agreement with the hypothesis that binary stars are distributed uniformly in these parameters for $0.1 \leq q \leq 1$. Since the probability of observing an event caused by a binary with very small ($d \leq 0.1r_E$) or very large ($d \geq 10r_E$) separation is negligible, it is impossible to check the wider range of separations using microlensing and the present database. For a “typical” event including binary in the Galactic disk the Einstein radius $r_E \approx 1$ a.u., so our approach probes the binary stars with separations of similar order of magnitude.

Of the planetary lenses only one (OGLE 2003-BLG-235/MOA 2003-BLG-53 – compare Bond *et al.* 2004) is a “strong case”. The other extreme mass ratio models of Paper I may be replaced by a less extreme mass ratio models and/or by a double source models. The event OGLE 2002-BLG-055 is not included in considerations because it is poorly constrained (Jaroszyński and Paczyński 2002) and may also be modeled as a double source event (Gaudi and Han 2004).

The distribution of binary events duration (Fig. 2) is systematically shifted to longer t_E as compared to single lens events, which can be partially explained as a result of the higher on average binary masses. The well pronounced peak of the binary duration distribution must be a fluctuation or some kind of selection effect, which makes the binary events with t_E between 64 and 100 days more likely to be discovered.

Some of the events of this study were also reported elsewhere. The event OGLE 2002-BLG-069 was observed by the PLANET collaboration and the caustic exit was monitored spectroscopically by VLT (Cassan *et al.* 2004) to probe the atmosphere of the source star – a G5III giant in Galactic bulge. The atmospheric study does not require the full binary lens model, which has not been published yet, so the direct comparison is not possible.

The event OGLE 2003-BLG-135 was also observed by the MOA group (Bond *et al.* 2001) and is named MOA 2003-BLG-21. More interesting is the event OGLE 2003-BLG-235/MOA 2003-BLG-53. The combined observations of OGLE and MOA were modeled by the two teams and reported as a planetary microlensing event set including the coverage of the second caustic crossing (Bond *et al.* 2004). The parameters of the best fit based on large data set including the coverage of the second caustic crossing (predicting $q = 0.0039$, $d = 1.12$, and $t_E = 61.5$) are in rough agreement with our results.

The event OGLE 2003-BLG-095 (treated here as an example of double source lensing) was modeled by Collinge (2004), who considers also the binary lens model of the event and the influence of the parallax effect. The double source models presented here and in his paper are similar.

The events OGLE 2003-BLG-170 and OGLE 2003-BLG-267 have well covered caustic crossings. The latter is also showing some effects of parallax and/or internal variability. The further study of these events may give some limits on the possible distances and masses of the binary lenses.

Acknowledgements. We thank Bohdan Paczyński for many helpful discussions and Shude Mao for the permission of using his binary lens modeling software. This work was supported in part by the Polish KBN grants 2-P03D-016-24 and 2-P03D-021-24, the NSF grant AST-0204908, and NASA grant NAG5-12212.

REFERENCES

- Abt, H.A. 1983, *Ann. Rev. Astron. Astrophys.*, **21**, 343.
 Alard, C. 2000, *Astron. Astrophys. Suppl. Ser.*, **144**, 363.
 Alard, C., and Lupton, R.H. 1998, *Astrophys. J.*, **503**, 325.
 Albrow, M.D., *et al.* 1999a, *Astrophys. J.*, **512**, 672.
 Albrow, M.D., *et al.* 1999b, *Astrophys. J.*, **522**, 1011.
 Albrow, M.D., *et al.* 1999c, *Astrophys. J.*, **522**, 1022.
 Alcock, C., *et al.* 2000, *Astrophys. J.*, **541**, 270.
 An, J.H., *et al.* 2002, *Astrophys. J.*, **572**, 521.
 Bennett, D., and Rhie, H. 1996, *Astrophys. J.*, **472**, 660.
 Blandford, R.D., and Narayan, R. 1992, *Ann. Rev. Astron. Astrophys.*, **30**, 311.
 Bond, I.A. *et al.* 2001, *MNRAS*, **327**, 868.
 Bond, I.A. *et al.* 2004, *Astrophys. J. Letters*, **606**, L155.
 Cassan, A. *et al.* 2004, *Astron. Astrophys.*, **419**, L1.
 Collinge, M.J. 2004, astro-ph/0402385.
 DiStefano, R., and Mao, S. 1996, *Astrophys. J.*, **457**, 93.
 Dominik, M. 1998, *Astron. Astrophys.*, **333**, L79.
 Dominik, M. 1999, *Astron. Astrophys.*, **341**, 943.
 Gaudi, B.S., and Gould, A. 1997, *Astrophys. J.*, **486**, 85.
 Gaudi, B.S., and Han, Ch. 2004, *Astrophys. J.*, submitted, astro-ph/0402417.
 Gould, A., and Loeb, A. 1992, *Astrophys. J.*, **396**, 104.
 Graff, D.S., and Gould, A. 2002, *Astrophys. J.*, **580**, 253.
 Jaroszyński, M. 2002, *Acta Astron.*, **52**, 39 (Paper I).
 Jaroszyński, M., and Paczyński, B. 2002, *Acta Astron.*, **52**, 361.
 Mao, S., and DiStefano, R. 1995, *Astrophys. J.*, **440**, 22.
 Mao, S., and Loeb, A. 2001, *Astrophys. J. Letters*, **547**, L97.
 Mao, S., and Paczyński, B. 1991, *Astrophys. J. Letters*, **374**, L37.
 Paczyński, B. 1986, *Astrophys. J.*, **304**, 1.
 Paczyński, B. 1996, *Ann. Rev. Astron. Astrophys.*, **34**, 419.
 Schneider, P., Ehlers, J., and Falco, E.E. 1992, "Gravitational Lenses", Springer, Berlin.
 Schneider, P., and Weiss, A. 1986, *Astron. Astrophys.*, **164**, 237.
 Trimble, V. 1990, *MNRAS*, **242**, 79.
 Udalski, A. 2003, *Acta Astron.*, **53**, 291.
 Udalski, A., *et al.* 1994a, *Astrophys. J. Letters*, **436**, L103.
 Udalski, A., Szymański, M., Kaluzny, J., Kubiak, M., Mateo, M., Krzemiński, W., and Paczyński, B. 1994b, *Acta Astron.*, **44**, 227.
 Woźniak, P.R. 2000, *Acta Astron.*, **50**, 421.
 Woźniak, P.R., and Paczyński, B. 1997, *Astrophys. J.*, **487**, 55.
 Woźniak, P.R., Udalski, A., Szymański, M., Kubiak, M., Pietrzyński, G., Soszyński, I., and Żebruń, K. 2001, *Acta Astron.*, **51**, 175.

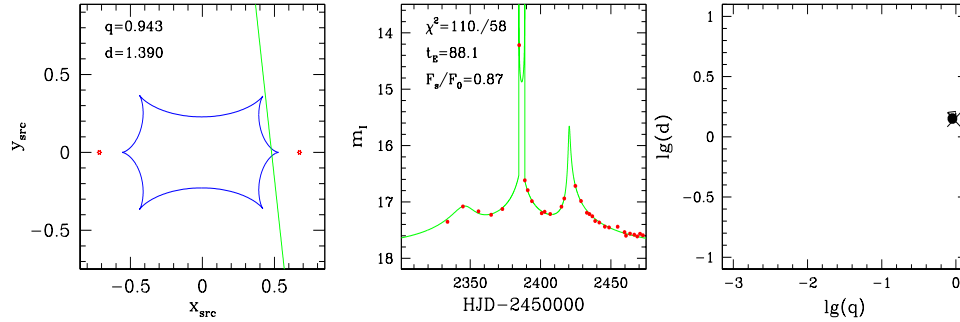
Appendix 1: Binary Lens Models of Candidate Events

Below we present the plots for the 24 events for which the binary lens modeling has been applied. Some of the models, especially cases interpreted as cusp approach events, are not well constrained. The majority of events modeled as cusp approaches have alternative double source models of similar quality, and are shown in Appendix 2.

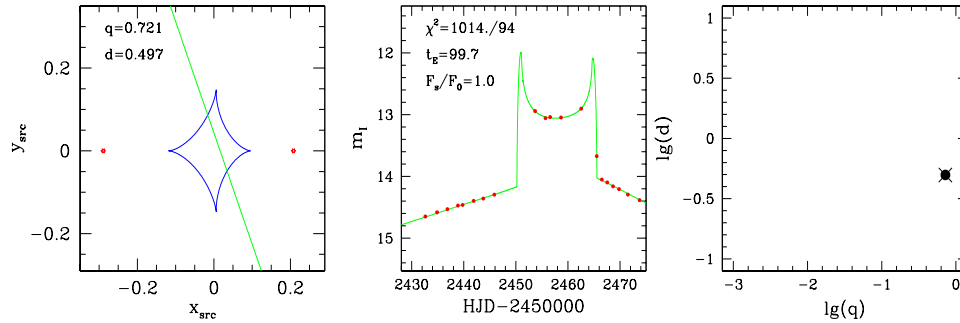
The events are ordered and named according to their position in the OGLE EWS database for seasons 2002 and 2003. For two events we also give their names in MOA database. Some events have more than one binary lens model of comparable fit quality (compare Table 1) which we show as the 1st, 2nd etc models.

Each case is illustrated with three panels. The most interesting part of the source trajectory, the binary and its caustic structure are shown in the left panel for the case considered. The labels give the q and d values. In the middle panel the part of the best fit light curve is compared with observations. The labels give the rescaled χ^2/DOF values, the Einstein time t_E in days and the source flux / base flux ratio. The diagram on the right shows the 68% and 99% confidence regions in the $\lg q$ - $\lg d$ plane. The location of the best fit is marked with a large dot, and the position of the fit illustrated in a given row – with a cross. In some cases the confidence regions are small and completely or partially hidden behind the dots.

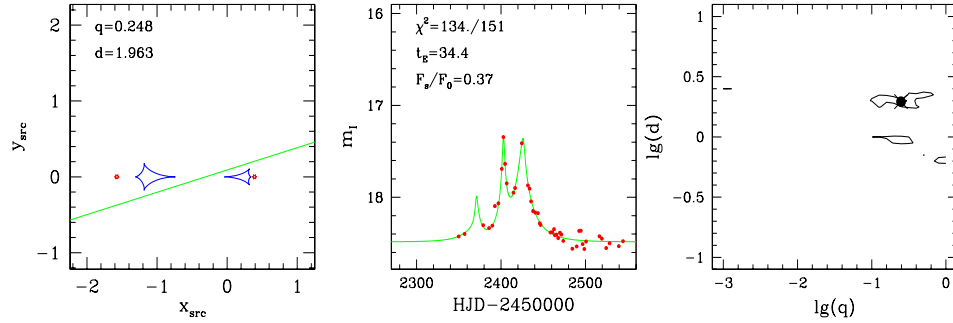
OGLE 2002-BLG-051



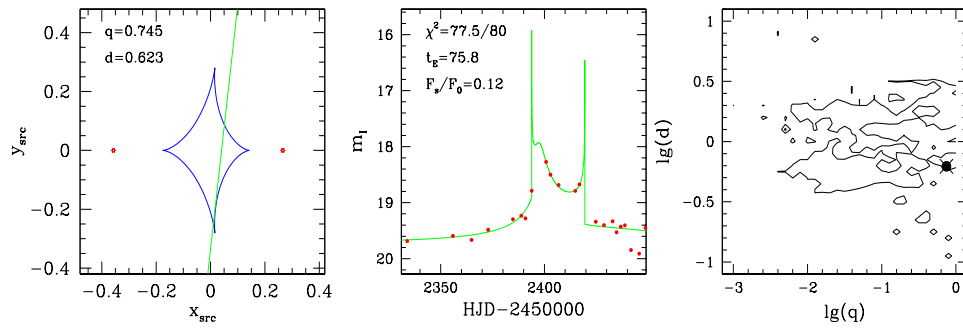
OGLE 2002-BLG-069



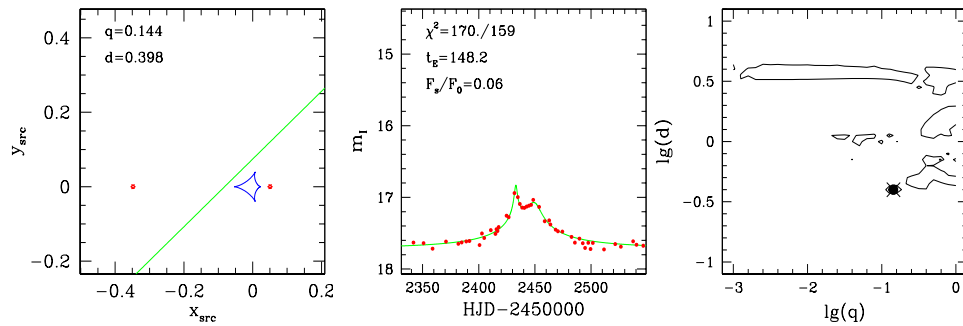
OGLE 2002-BLG-099



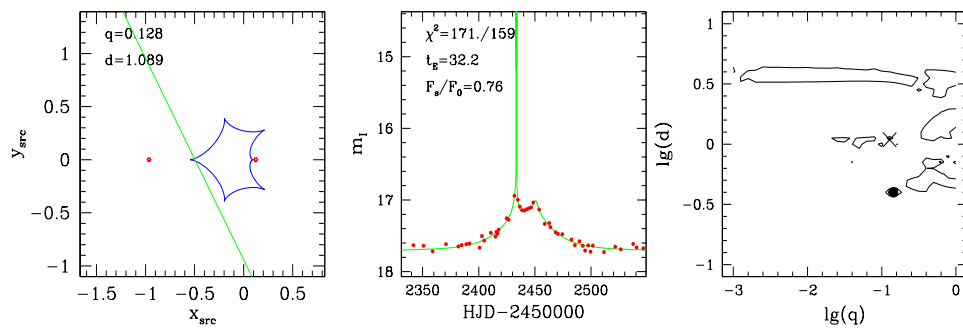
OGLE 2002-BLG-114



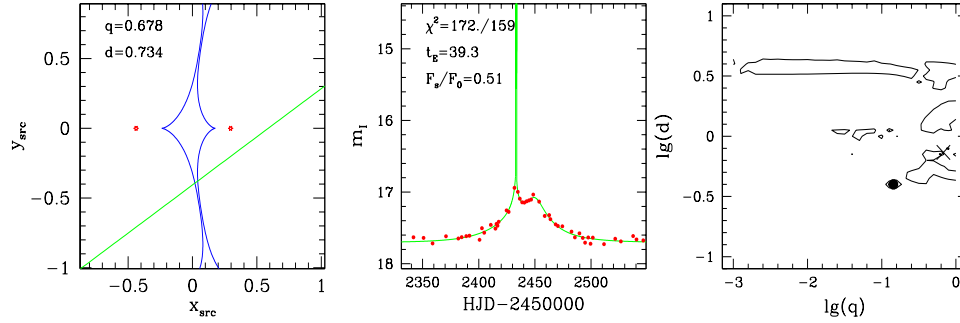
OGLE 2002-BLG-135 (1st model)



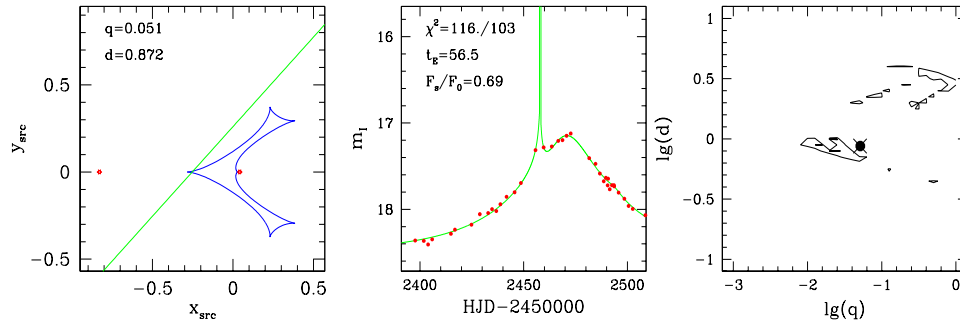
OGLE 2002-BLG-135 (2nd model)



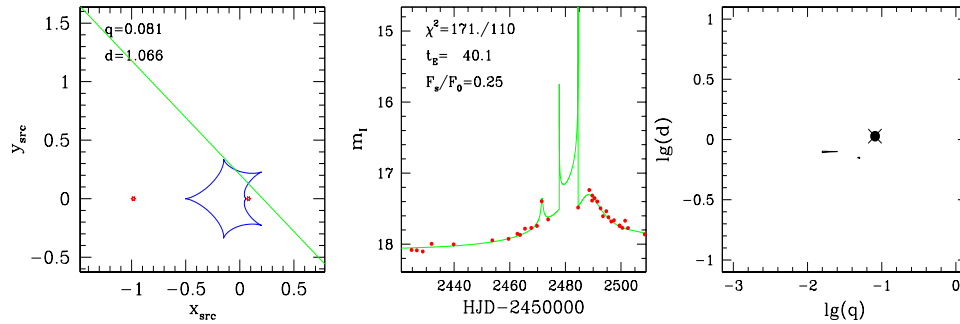
OGLE 2002-BLG-135 (3rd model)



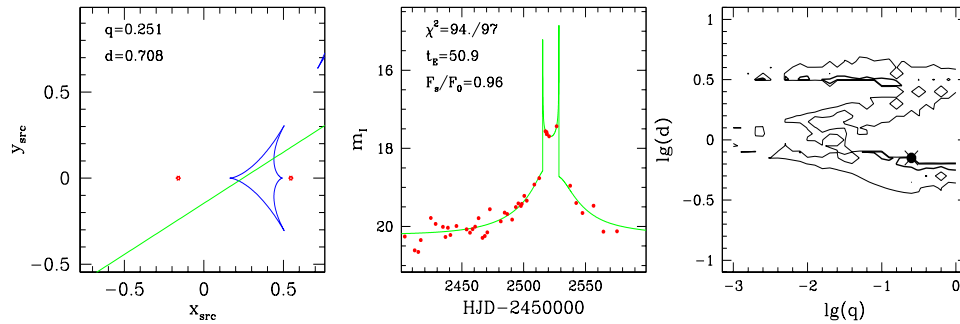
OGLE 2002-BLG-158

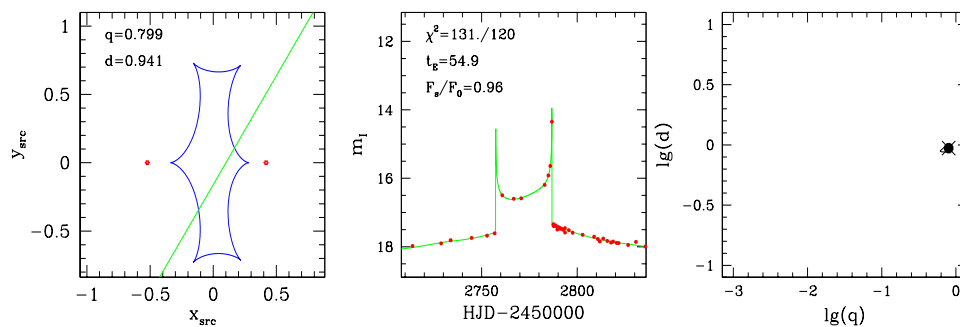
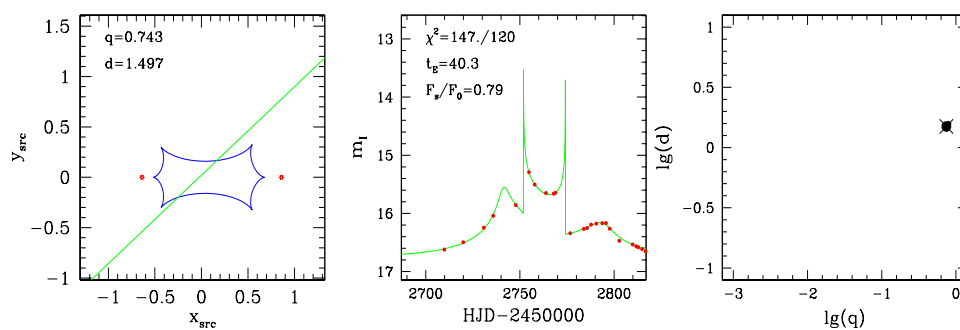
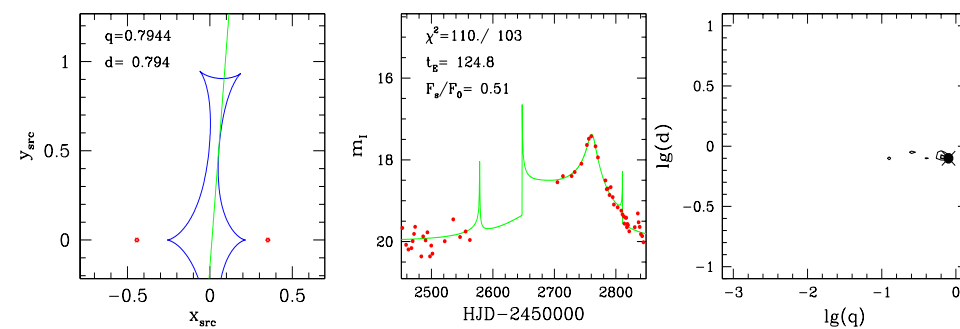
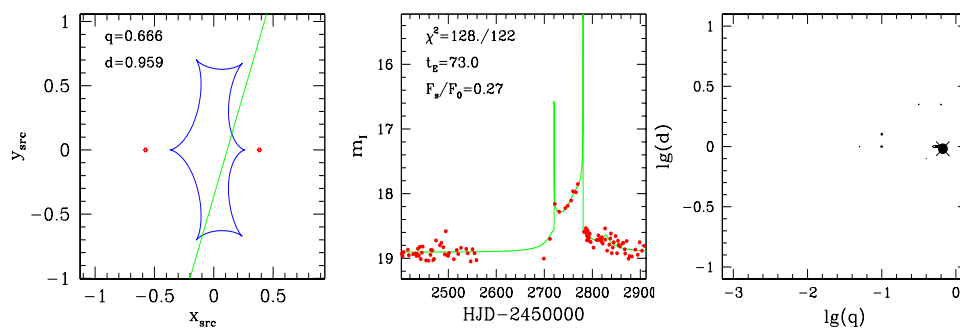


OGLE 2002-BLG-256

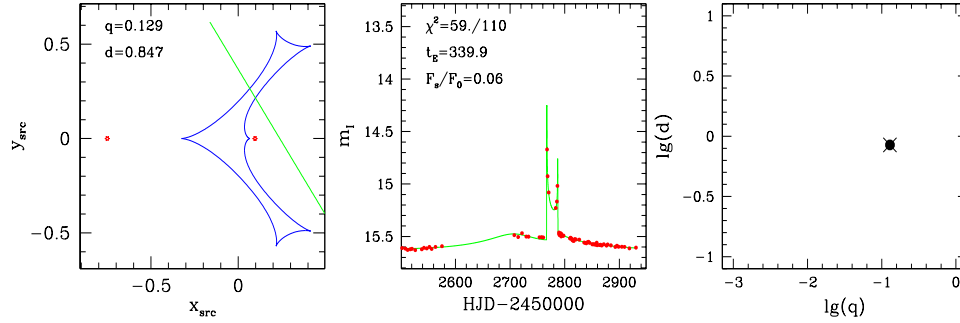


OGLE 2002-BLG-321

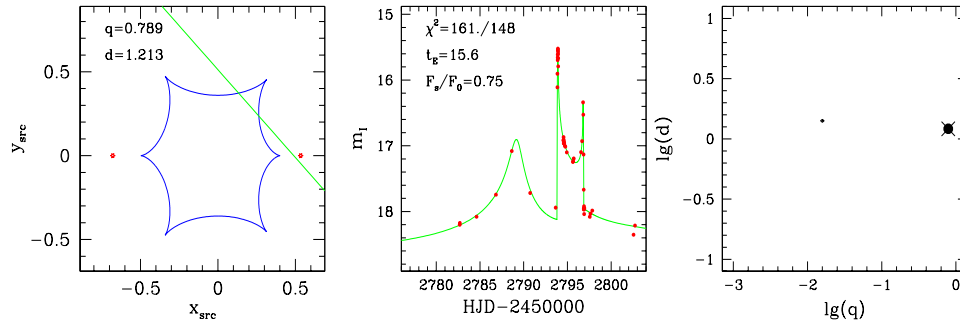


OGLE 2003-BLG-021**OGLE 2003-BLG-056****OGLE 2003-BLG-084****OGLE 2003-BLG-124**

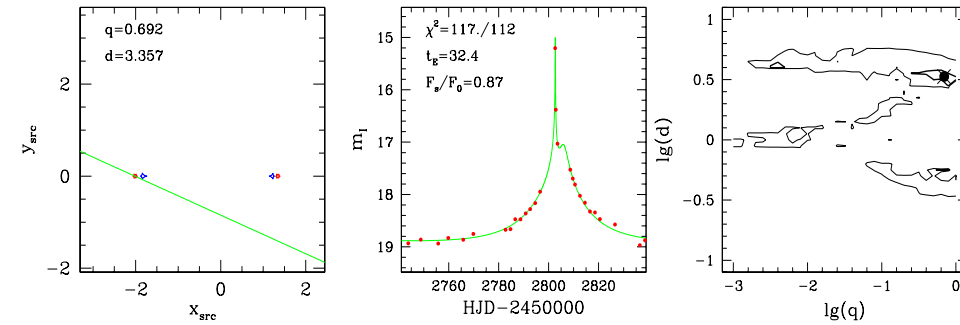
OGLE 2003-BLG-135 / MOA 2003-BLG-21



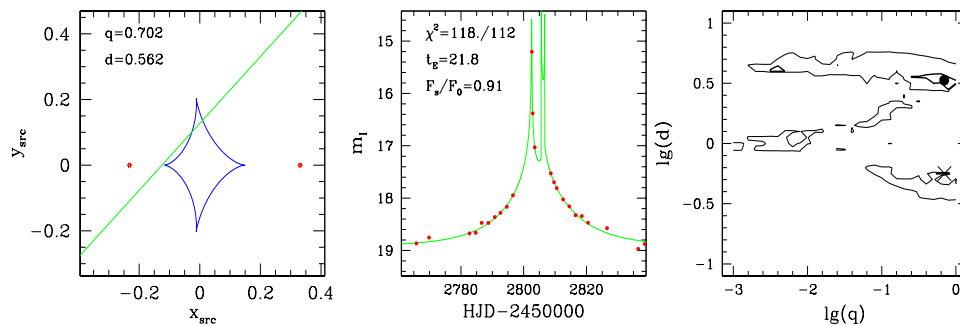
OGLE 2003-BLG-170



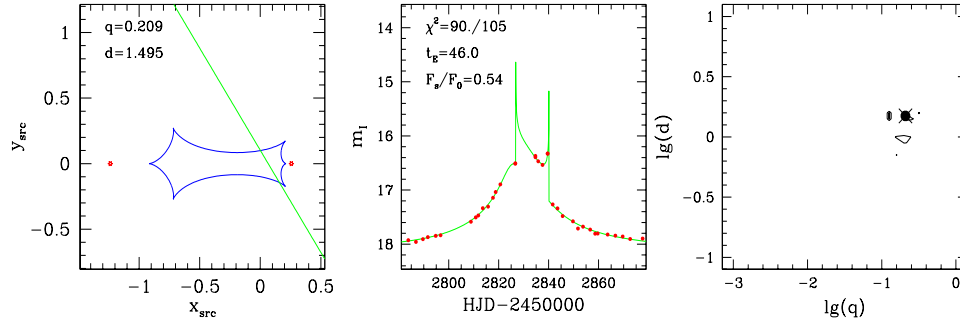
OGLE 2003-BLG-194 (1st model)



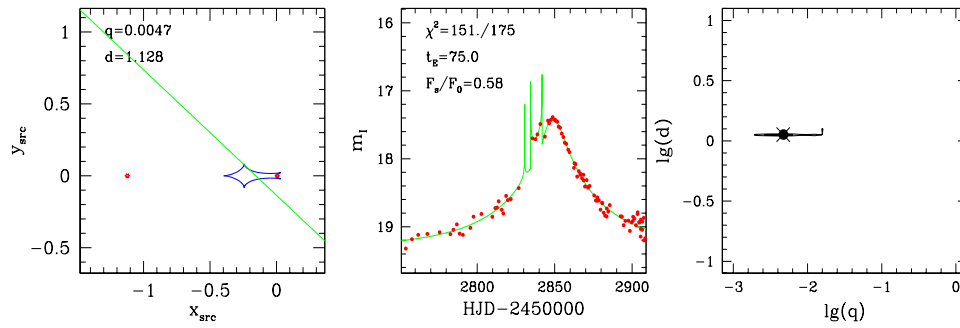
OGLE 2003-BLG-194 (2nd model)



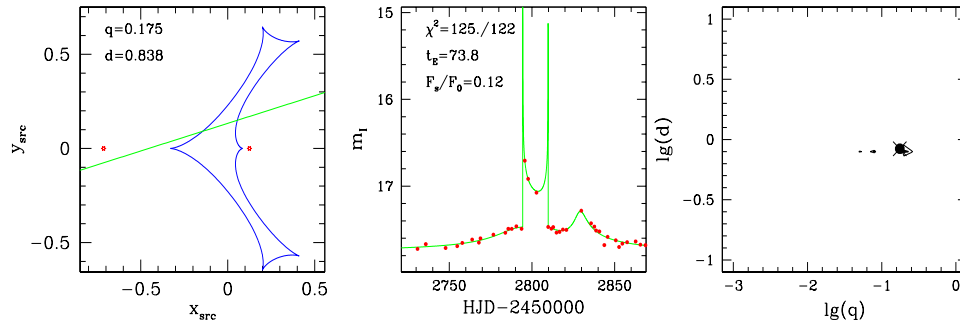
OGLE 2003-BLG-200



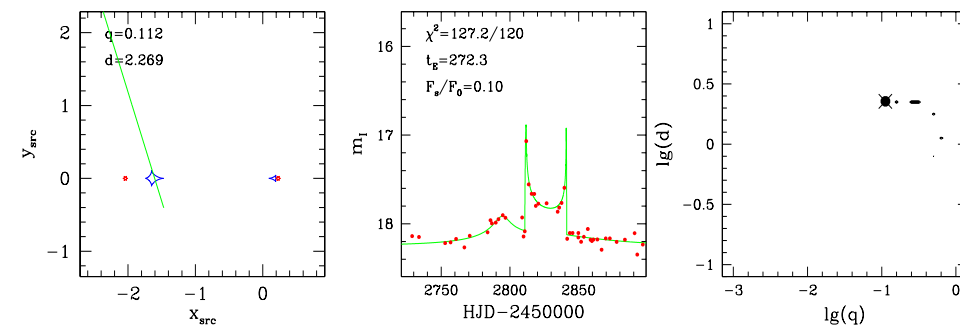
OGLE 2003-BLG-235 / MOA 2003-BLG-53



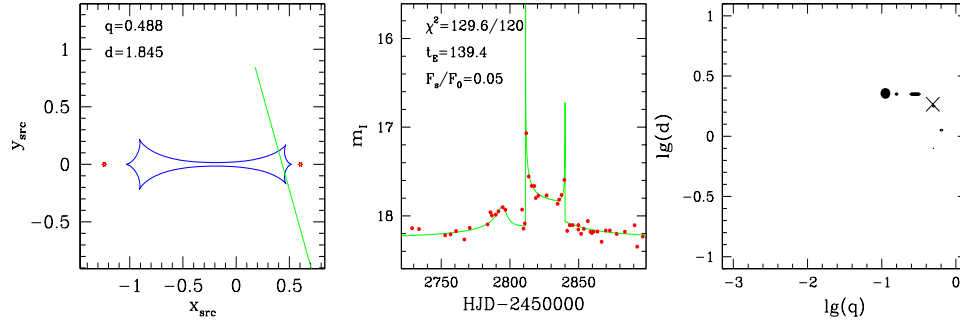
OGLE 2003-BLG-236



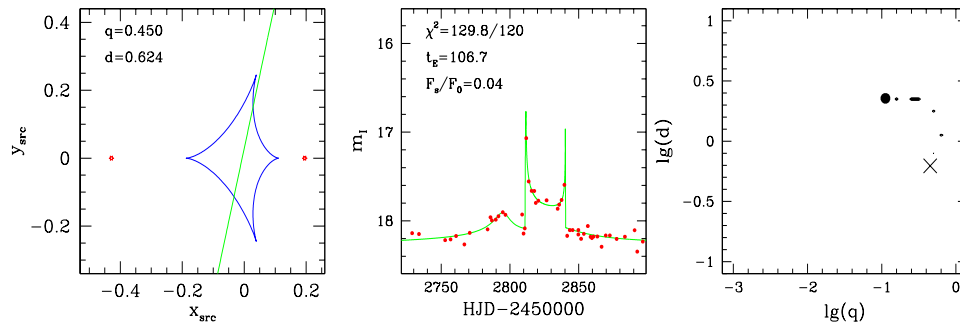
OGLE 2003-BLG-260 (1st model)



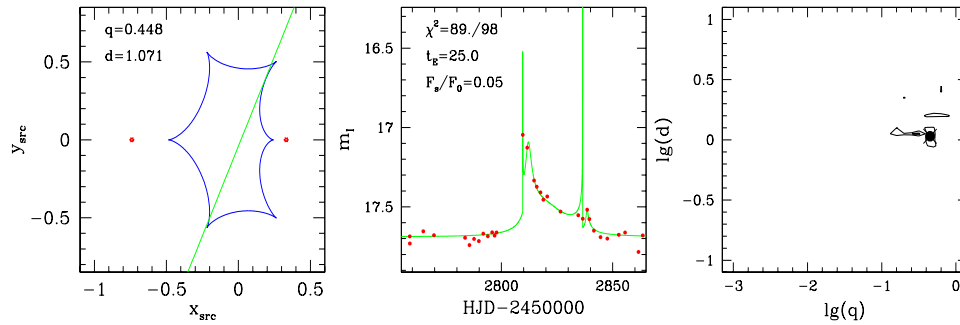
OGLE 2003-BLG-260 (2nd model)



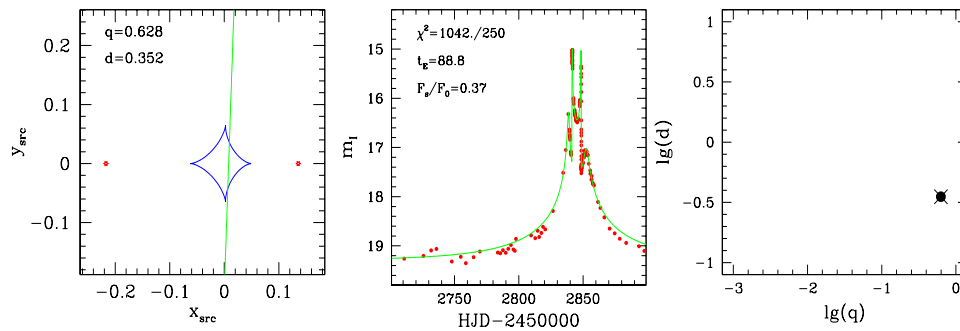
OGLE 2003-BLG-260 (3rd model)



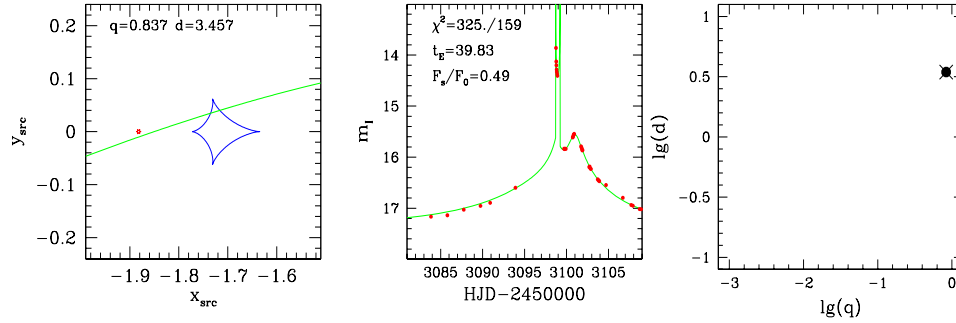
OGLE 2003-BLG-266



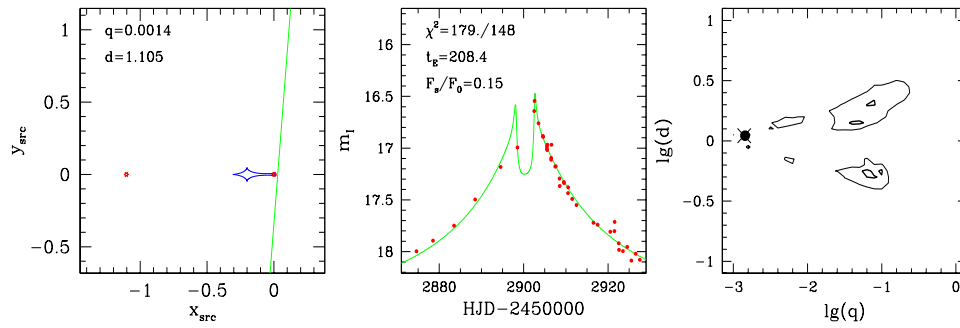
OGLE 2003-BLG-267



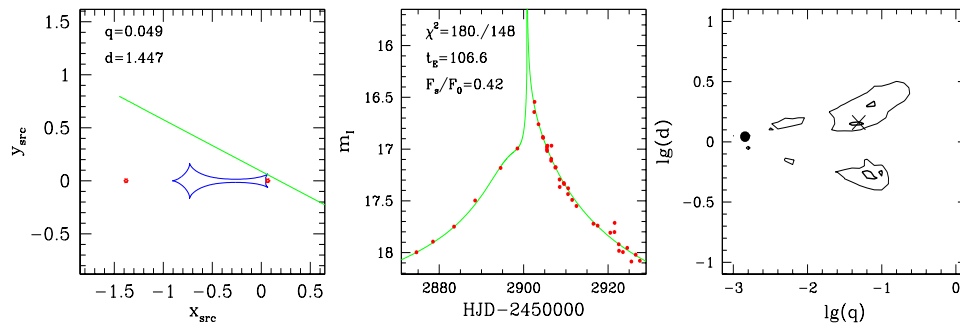
OGLE 2003-BLG-291



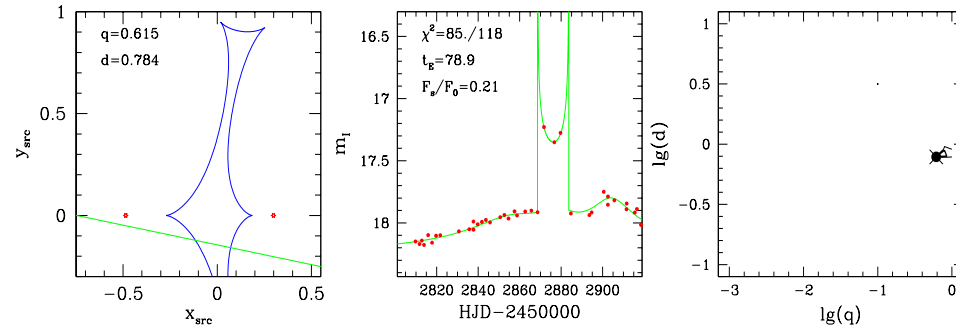
OGLE 2003-BLG-340 (1st model)



OGLE 2003-BLG-340 (2nd model)



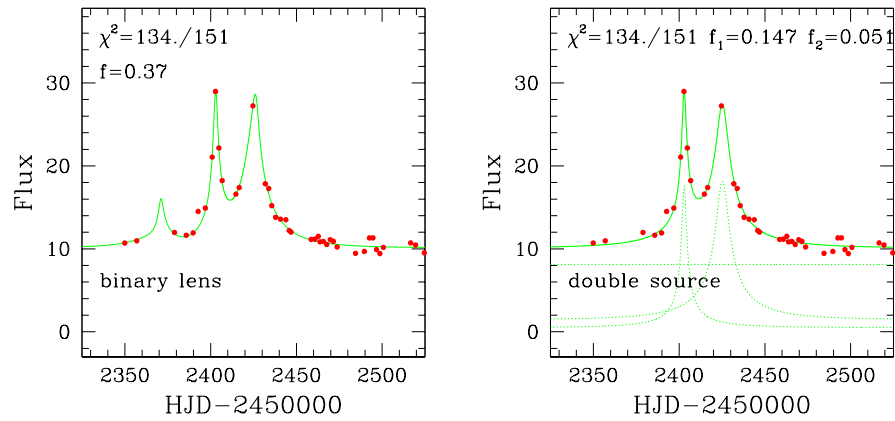
OGLE 2003-BLG-380



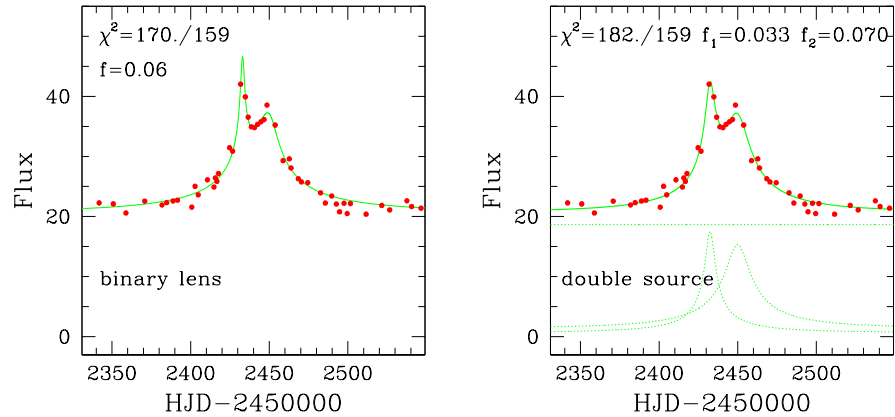
Appendix 2: Ambiguous Binary Lens / Double Source Events

In the following we show events which have two kinds of models of comparable quality. The binary lens models are shown on the left and double source models – on the right. Since the flux of a double source is a linear combination of its components and the blend, we use flux units in the plots. (One flux unit corresponds to $I=21$ mag.) The resulting light curves are shown as thick solid lines, while observations are marked as dots. For the double source models we also show the light curves of the contributing components and of the blend using thin dotted lines. (More information relating to the binary models of the events can be found in Appendix 1.)

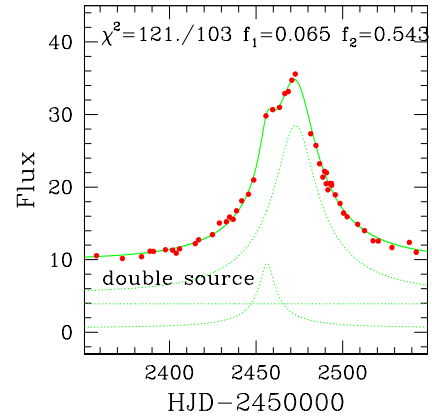
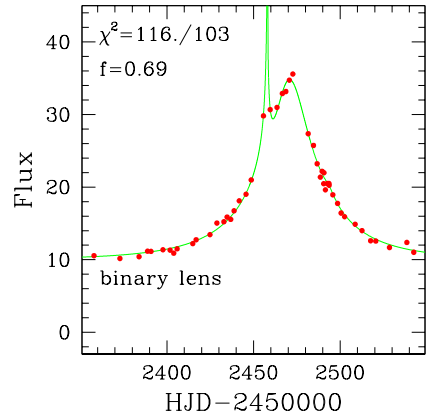
OGLE 2002-BLG-099



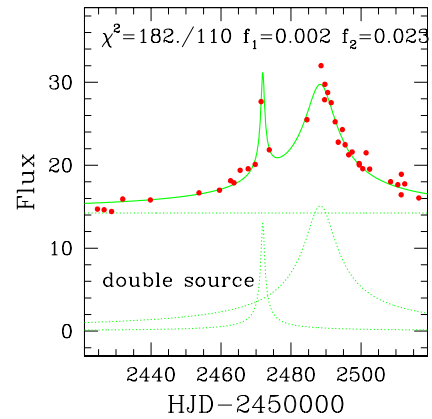
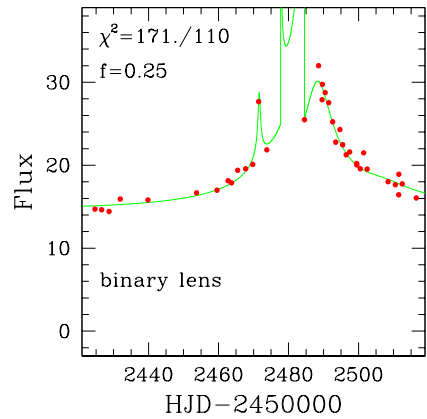
OGLE 2002-BLG-135



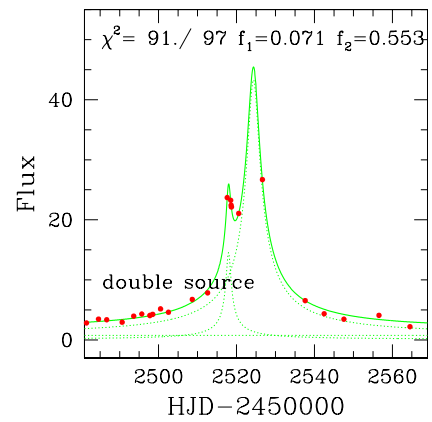
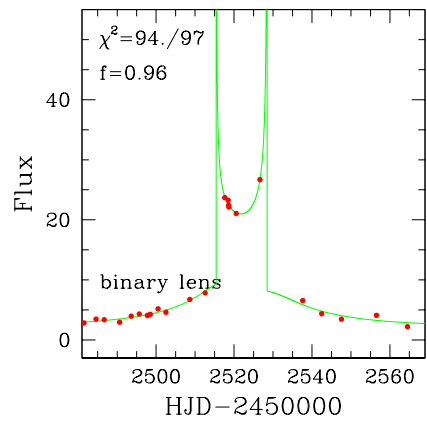
OGLE 2002-BLG-158



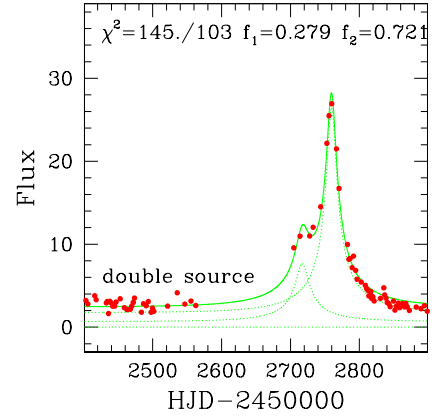
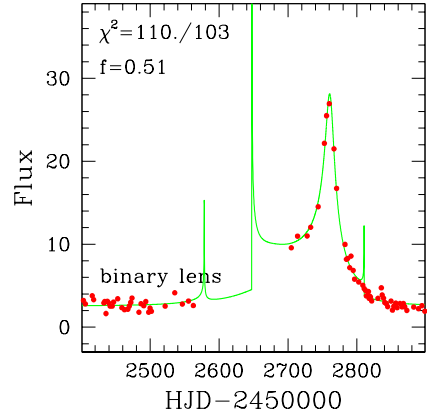
OGLE 2002-BLG-256



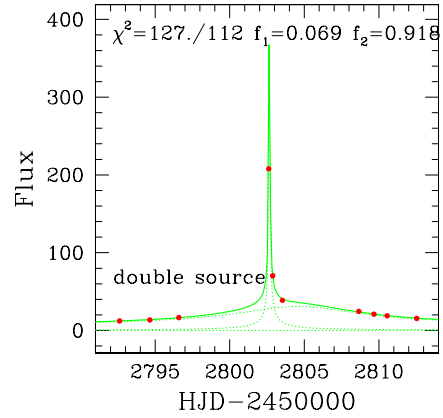
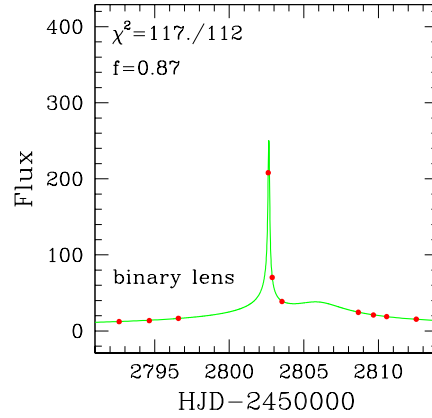
OGLE 2002-BLG-321



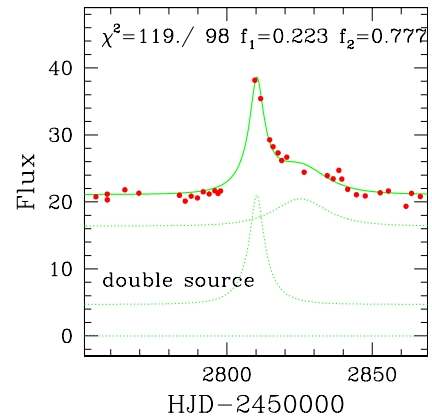
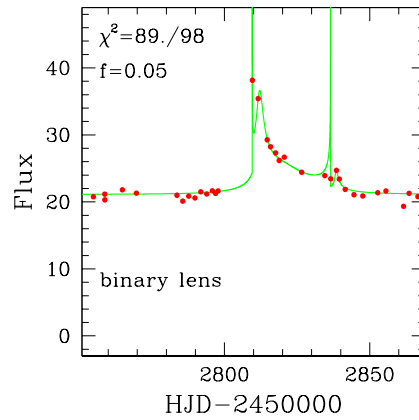
OGLE 2003-BLG-084

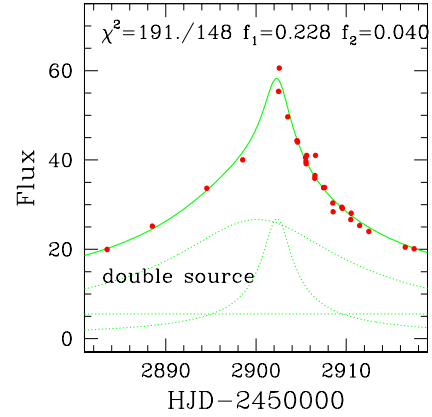
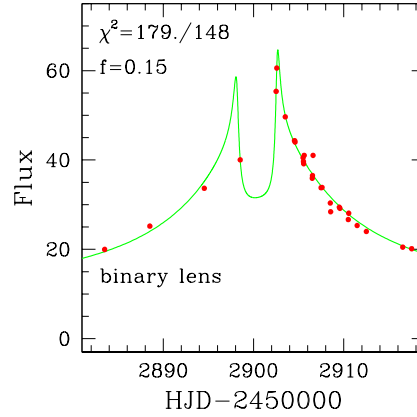


OGLE 2003-BLG-194

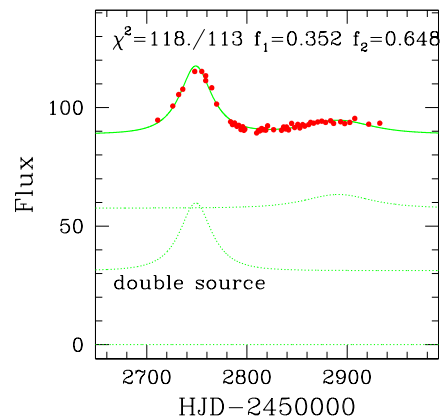
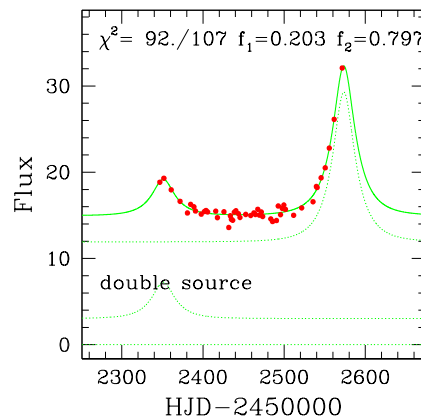


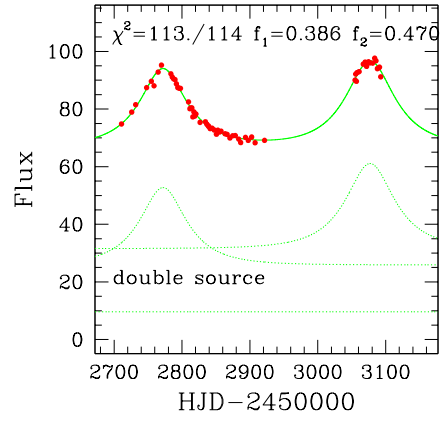
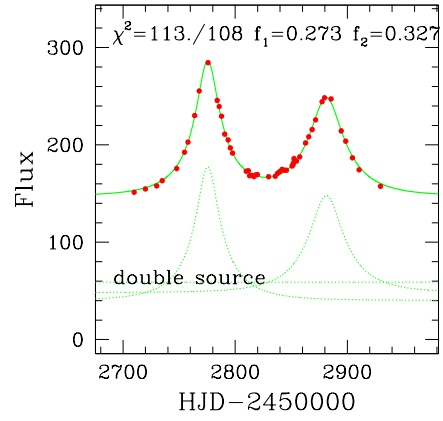
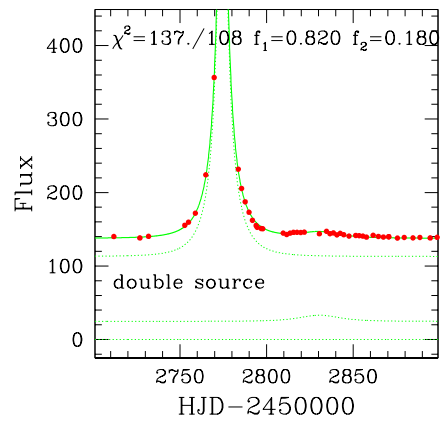
OGLE 2003-BLG-266



OGLE 2003-BLG-340**Appendix 3: Well Separated Double Source Events**

We also show a few unambiguous double source events – cases, where the source components are well separated which results in two peaks in the light curves, each resembling closely a single source / single lens event.

OGLE 2002-BLG-018**OGLE 2003-BLG-063**

OGLE 2003-BLG-067**OGLE 2003-BLG-095****OGLE 2003-BLG-126**

Appendix 4: Rejected Event

The following candidate event has been rejected: we could not find a binary lens model which would (at least qualitatively) fit its light curve.

OGLE 2003-BLG-303